

## Chapter 39

# PET Imaging of the Impact of Extracellular pH and MAP Kinases on the *p*-Glycoprotein (Pgp) Activity

Oliver Thews, Wolfgang Dillenburg, Frank Rösch, and Marco Fellner

**Abstract** The functional activity of *p*-glycoprotein (Pgp) can be increased in vitro by an extracellular acidosis via activation of MAP kinases (p38, ERK1/2). In order to study these effects in vivo a new <sup>68</sup>Ga-labeled PET tracer was developed which serves as a substrate of the Pgp and therefore indirectly mirrors the Pgp activity. For in vivo studies, experimental tumors were imaged under acidic conditions (inspiratory hypoxia, injection of lactic acid) and during inhibition of MAP kinases in a  $\mu$ -PET system. In vitro, [<sup>68</sup>Ga]MFL6.MZ showed an accumulation within the cells of about 20% which was increased to 30% by Pgp inhibition. In solid tumors a marked tracer uptake was observed showing spatial heterogeneity. When the tumors were acidified, the PET tracer accumulation was reduced by 20–30%. Changing the inspiratory O<sub>2</sub>-fraction to 8% led dynamically to a decrease in pH and in parallel to a reduced tracer concentration. Inhibition of the p38 pathway reduced the Pgp transport rate. The new <sup>68</sup>Ga-labeled tracer is suitable for PET imaging of the tissue Pgp activity. In vivo imaging reveals that an acidosis activates the Pgp markedly, a mechanism in which the p38-MAPK pathway seems to play an important role.

**Keywords** *p*-Glycoprotein • Acidosis • MAP kinases • PET • <sup>68</sup>Ga

---

This study forms part of the doctoral thesis of Wolfgang Dillenburg.

O. Thews (✉)

Julius-Bernstein Institute of Physiology, University of Halle-Wittenberg,  
Magdeburger Str. 6, 06112 Halle (Saale), Germany  
e-mail: oliver.thews@medizin.uni-halle.de

W. Dillenburg

Institute of Physiology and Pathophysiology, University Medicine Mainz, Mainz, Germany

F. Rösch • M. Fellner

Institute of Nuclear Chemistry, University of Mainz, Mainz, Germany

## 22 1 Introduction

23 Solid tumors show several pronounced differences as compared to normal tissues  
24 with respect to physiological characteristics at the cellular and tissue level. As a  
25 consequence of insufficient tumor perfusion [1] there is inadequate oxygen delivery  
26 with forced anaerobic metabolism resulting in an increased lactic acid formation [2]  
27 and extracellular acidosis [1]. Numerous studies have demonstrated that the abnormal  
28 physiological microenvironment reduces the cytotoxicity of chemotherapeutic  
29 drugs [3].

30 On the other hand, reduced chemosensitivity may result from drug transporters  
31 which actively pump amphiphilic xenobiotics out of the cell [4]. Modulation of  
32 these drug transporters (e.g., by inhibitors) can modify the cytotoxic efficacy of  
33 chemotherapy [5]. The best studied member of the ABC-transporter family is the  
34 *p*-glycoprotein (Pgp) responsible for a multidrug-resistant phenotype of many human  
35 tumors. Besides constitutional differences in the Pgp expression of tumor entities or  
36 cell lines, the expression as well as the functional activity of the transporter has been  
37 shown to be regulated. In vitro studies [6, 7] demonstrated that lowering the extra-  
38 cellular pH to 6.5 functionally increases the Pgp activity and by this reduces the  
39 cytotoxicity of chemotherapeutics which are a substrate of the *p*-glycoprotein. In  
40 vivo it was shown that lowering the tumor pH by forcing anaerobic glycolysis  
41 decreases the cytotoxicity of daunorubicin [6] which could be attributed to an acido-  
42 sis-induced activation of the Pgp. However, in these experiments the Pgp transport  
43 rate itself could not be measured in vivo. The study also revealed that MAP kinases  
44 (p38, ERK1/2) are a signaling pathways responding to extracellular pH and that  
45 activate Pgp [6]. Inhibition of p38 or ERK1/2 reduced the Pgp activity in vitro.

46 From these results, there is strong evidence that extracellular acidosis function-  
47 ally increases the Pgp activity via a p38-mediated pathway in vivo [6]. With func-  
48 tional imaging such as PET it might be possible to measure the functional Pgp  
49 activity noninvasively and to confirm the impact of extracellular acidosis on drug  
50 transport as well as to identify the role of MAP kinases in the signaling pathway  
51 in vivo.

## 52 2 Material and Methods

### 53 2.1 PET Tracer and Tumor Model

54 For functional Pgp imaging, six tracers (MFL1.MZ-MFL6.MZ) were synthesized  
55 which consist of hexadentate Schiff-bases labeled with the positron emitter  $^{68}\text{Ga}$   
56 ( $T_{1/2} = 67.7$  min,  $\beta^+$  branching = 89 %).  $^{68}\text{Ga}$  was eluted from a  $^{68}\text{Ge}/^{68}\text{Ga}$  generator  
57 [8] with 10 mL HCl and on line-immobilized on an acidic cation exchanger. [AU1]  
58 Labeling was performed with 20  $\mu\text{L}$  of each ligand solution (1 mg/mL in EtOH,  
59 30 nmol). Radiochemical labeling yield and complex formation were determined by

thin layer chromatography (TLC). For injection the tracer pH was adjusted to 7.4 with NaOH and diluted with isotonic saline. The tracers themselves are substrates of the Pgp and are actively pumped out of the cell. The intratumoral concentration reflects therefore inversely the Pgp activity.

In all experiments the subline AT1 of the R3327 Dunning prostate carcinoma was used which functionally expresses the *p*-glycoprotein [7]. Cells were grown in RPMI 1640 medium (+10 % fetal calf serum) and passaged once per week. Solid carcinomas of this cell line were heterotopically induced by injection of AT1 cells (0.4 mL approximately  $10^4$  cells/ $\mu$ L) subcutaneously into the dorsum of the hind foot. Tumors were used when they reached a volume of between 1.0 and 2.0 mL approximately 10–14 days after tumor cell inoculation.

## 2.2 Acidosis Model and Tumor Treatment

In order to dynamically change the extracellular pH of the tumors, the inspiratory gas mixture was changed from pure oxygen (100 % O<sub>2</sub>) starting 10 min prior to the PET tracer injection to a hypoxic gas containing 92 % N<sub>2</sub> + 8 % O<sub>2</sub> at 15 min after tracer injection (i.e., during the  $\mu$ -PET measurement). It was continued until the end of the  $\mu$ -PET measurement at 60 min. In parallel, the extracellular pH was measured with steel-shafted pH glass electrodes (type MI-418B, Microelectrodes Inc, Bedford NH, USA) with an outer diameter of 800  $\mu$ m inserted into the center of the tumor. Before and after the PET imaging, the electrode was calibrated and pH measurements were corrected for signal shift.

In a second series the extracellular tumor space was acidified by small amounts of lactic acid injected directly intratumorally. Therefore, 50  $\mu$ L of a 0.222 mM solution of lactic acid were injected in the tumor tissue at a depth of 2–3 mm about 5–10 min prior to the tracer application. The same amount of a 0.222 mM sodium lactate solution was applied in the contralateral tumor and this tumor served as intra-individual control.

In order to inhibit different MAP kinase pathways specific inhibitors (SB203580 and U0126 for inhibition of p38 and ERK1/2, respectively) were injected intratumorally. Therefore, inhibitors were dissolved in DMSO at a concentration of 1 mmol/L and tumors were treated with a single injection of a small amount (20  $\mu$ L) of these inhibitors 5–10 min prior to the PET measurements. The tumor on the contralateral hind foot was treated with 20  $\mu$ L DMSO alone and served as intra-individual control.

## 2.3 $\mu$ -PET Imaging

The  $\mu$ -PET imaging was performed on a microPET Focus 120 small animal PET (Siemens/Concorde, Knoxville, USA). During measurements the anaesthetized

97 (pentobarbital 40 mg/kg, i.p.) rats were placed in supine position and breathed room  
 98 air spontaneously through a tracheal tube. After a 15 min transmission scan with an  
 99 external  $^{57}\text{Co}$  source, dynamic PET studies were acquired in 2D mode. The  
 100 radiotracer was administered as a bolus injection (0.4–0.7 mL, mean activity  
 101  $44.0 \pm 1.5$  MBq) via a catheter placed in the left jugular vein. Time activity curves  
 102 were obtained with varying time frames (1–5 min) for a total measuring interval of  
 103 60 min. Volumes-of-interest (VOIs) were defined for tumor and reference tissue in  
 104 the field of view (testis). Ratios of tumor to reference tissue were calculated from  
 105 integral image between 10 and 60 min after tracer injection.

### 106 3 Results

107 In order to measure the cellular uptake of the  $^{68}\text{Ga}$ -Schiff base complexes, AT1 cells  
 108 were incubated with the tracer in the presence or absence of the Pgp inhibitor verapamil  
 109 (VPL) for 30 min after which the suspension was centrifuged and the activity  
 110 in the cells and in the supernatant was determined. Figure 39.1a shows the fraction  
 111 of  $^{68}\text{Ga}$ -complexes detected inside the cells for all tracers. Tracers MFL2.MZ,  
 112 MFL5.MZ, and MFL6.MZ were found to be substrates of Pgp since the active efflux  
 113 could be inhibited by VPL resulting in a statistically significant higher intracellular  
 114 concentration (Fig. 39.1a; e.g.,  $178 \pm 5$  % for  $^{68}\text{Ga}$ ]MFL2.MZ and  $144 \pm 3$  % for  
 115  $^{68}\text{Ga}$ ]MFL6.MZ). From these in vitro experiments it became evident that  $^{68}\text{Ga}$ ]  
 116 MFL2.MZ and  $^{68}\text{Ga}$ ]MFL6.MZ showed the best compromise of good passive  
 117 uptake into the cells and pronounced Pgp-mediated efflux inhibitable by VPL.  
 118 Subsequently, both these tracers were used in PET experiments with tumor-bearing  
 119 rats. Figure 39.1b shows the averaged activity in tumor and testes indicating that  
 120  $^{68}\text{Ga}$ ]MFL6.MZ is strongly accumulated in the tumors resulting in a three-times

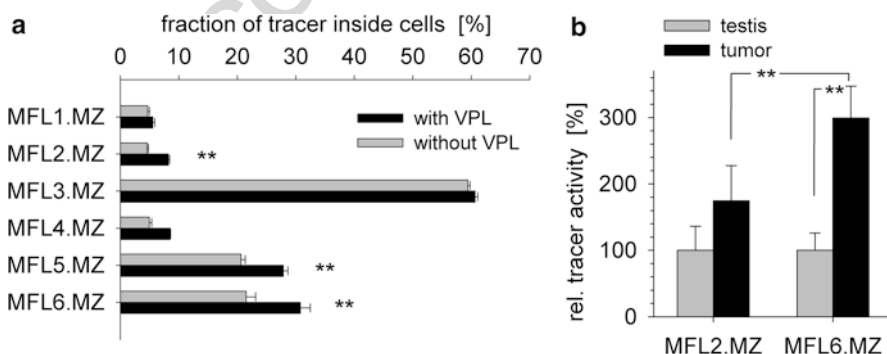


**Fig. 39.1** (a) In vitro accumulation of various  $^{68}\text{Ga}$ -labeled tracers in AT1 cells in the presence and absence of verapamil (VPL). (b) In vivo uptake of two tracers in AT1 tumors and a reference tissue (testis). Values are expressed as means  $\pm$  SEM; (double asterisk)  $p < 0.01$ ;  $n = 3-12$

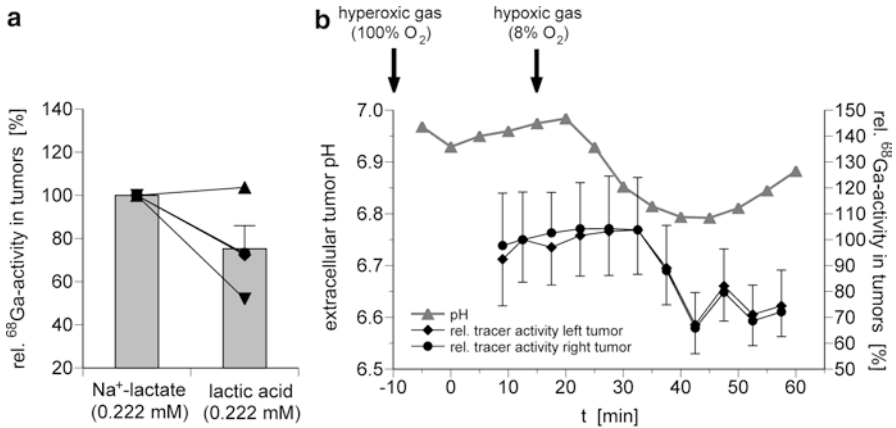


**Fig. 39.2** (a) Intratumoral [<sup>68</sup>Ga]MFL6.MZ concentration in tumors treated with lactic acid (50  $\mu$ L, 0.222 mM) or with an equivalent volume of Na<sup>+</sup>-lactate. Each line represents one individual animal with two tumors on each hind foot. Columns represent means  $\pm$  SEM of all experiments. (b) Extracellular pH and [<sup>68</sup>Ga]MFL6.MZ concentration during change of the inspiratory O<sub>2</sub>-fraction

higher concentration as compared to the reference tissue whereas [<sup>68</sup>Ga]MFL2.MZ is enriched by only 74 %. Therefore, [<sup>68</sup>Ga]MFL6.MZ was chosen for further experiments.

As a weak indication of a pH dependency of Pgp-mediated transport the extracellular pH and the tracer concentration were analyzed in tumors of different volume. A clear inverse correlation was found between the pH and tumor volume ( $r = -0.941$ ; data not shown) as well as between tracer concentration (inversely indicating the Pgp activity) and tumor volume ( $r = -0.550$ ; data not shown). Direct injection of lactic acid into one tumor (and Na<sup>+</sup>-lactate in the contralateral tumor) showed a markedly reduced tracer concentration in most of experiments (Fig. 39.2a) indicating a higher Pgp transport rate. Figure 39.2b illustrates an experiment where the pH was dynamically reduced during the imaging period by inspiratory hypoxia. Changing the inspiratory gas mixture from 100 to 8 % O<sub>2</sub> 15 min after tracer injection reduced the pH from 6.95 to values around 6.8 (Fig. 39.2b, triangles). With a slight delay of 10 min the intratumoral tracer concentration decreased by 25–30 % in both tumors.

Figure 39.3a illustrates an example where in the right tumor the p38 inhibitor SB203580 was injected whereas the left tumor received only DMSO. The right tumor shows a much higher tracer concentration indicating a reduced Pgp activity. This effect was seen in all animals (Fig. 39.3b). On average, the SB203580-treated tumors showed a more than 70 % higher tracer concentration than the contralateral control tumors. Inhibition of the ERK1/2 pathway by U0126 had only a minor effect on the Pgp activity (increase of the tracer concentration by only 29 %; data not shown).

121  
122  
123  
124  
125  
126  
127  
128  
129  
130  
131  
132  
133  
134  
135  
136  
137  
138  
139  
140  
141  
142  
143  
144

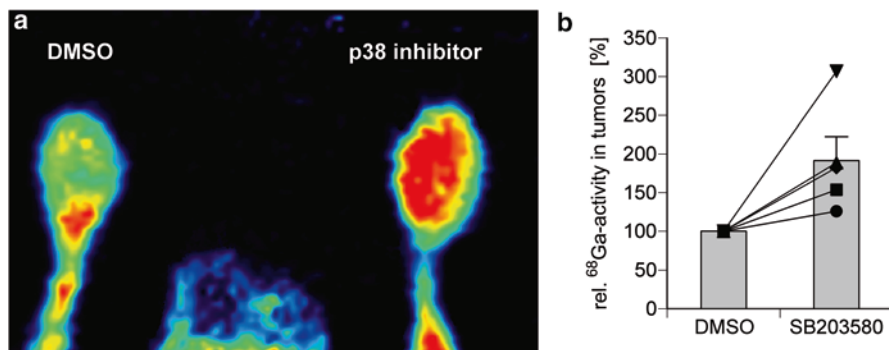


**Fig. 39.3** (a) Example of [ $^{68}\text{Ga}$ ]MFL6.MZ accumulation in AT1 tumors. In the right tumor 20  $\mu\text{L}$  of a p38 MAPK inhibitor (SB203580) was injected whereas the contralateral tumor received the same volume of the vehicle (DMSO). (b) Relative [ $^{68}\text{Ga}$ ]MFL6.MZ concentration in all tumors treated with the p38 inhibitor or with DMSO. Each line represents one individual animal with tumors on each hind foot. Columns represent means  $\pm$  SEM of all experiments

## 145 4 Discussion

146 A suitable PET tracer for measuring the Pgp transport rate should fulfill two fea-  
 147 tures: (1) it should enter the cell easily (by passive diffusion) and (2) the tracer  
 148 should be a substrate of the Pgp and this transport should be inhibitable by Pgp  
 149 inhibitors. All tracers show high cellular uptake but with marked concentration dif-  
 150 ferences. Taking into account the volume fraction of the cells ( $\sim 0.3\%$ ) the concen-  
 151 tration ratio between cells and medium was approximately 16:1 for most of the  
 152 tracers but  $\sim 90:1$  for [ $^{68}\text{Ga}$ ]MFL3.MZ which is the most lipophilic compound.  
 153 Since the intracellular concentration depends on the Pgp activity, the ratio of cellu-  
 154 lar tracer concentration in the presence and absence of verapamil could be used as  
 155 an indicator of the Pgp-mediated efflux [9]. This ratio was  $\sim 1.2\text{--}1.8$  for most tracers  
 156 (Fig. 39.1a) but for the lipophilic tracer [ $^{68}\text{Ga}$ ]MFL3.MZ Pgp inhibition had practi-  
 157 cally no impact. The uptake measurements in vivo correspond well with the in vitro  
 158 data as indicated by a higher tumor concentration of the tracer [ $^{68}\text{Ga}$ ]MFL6.MZ  
 159 compared to [ $^{68}\text{Ga}$ ]MFL3.MZ.

160 With this tracer  $\mu$ -PET images were analyzed after acidifying the tumor tissue by  
 161 direct injection of lactic acid. Since the interstitial fluid pressure is elevated in many  
 162 human malignancies, the injection of even a small fluid volume of lactic acid into  
 163 the tissue may somehow disturb tumor microcirculation. For this reason it cannot be  
 164 excluded that the direct injection may reduce tumor perfusion locally and by this  
 165 limit the tracer transport. For this reason, the contralateral tumor of each animal  
 166 served as an intra-individual control by injecting the same volume of an equimolar  
 167  $\text{Na}^+$ -lactate solution leading to a comparable increase of the interstitial hydrostatic  
 168 pressure. The comparison of the tracer concentration in both tumors therefore  
 169 reflects solely the impact of the lower pH on Pgp activity.

The second method for acidifying the extracellular space was to force anaerobic glycolysis leading to an increased endogenous formation of lactic acid. Breathing a hypoxic gas mixture with 8 % oxygen is suitable to markedly lower the tumor- $pO_2$  [10] and to reduce the tumor pH [6]. In the present study hypoxia led to decrease in pH followed by an increase in Pgp activity resulting in a lower tracer accumulation (Fig. 39.2a). The increase of pH 30 min after the onset of the hypoxic breathing remains unclear at the moment. Perhaps changes in the blood pressure or a hypoxia-induced vasodilation led to an increase in tumor perfusion and by this to a better oxygen supply.

Previous *in vitro* data revealed that MAP kinases (p38, ERK1/2) play a relevant role for signal transduction in the acidosis-induced Pgp activation [6]. The present study clearly shows that MAP kinases are also important for the Pgp transport activity *in vivo*. Inhibition of p38 by SB203580 increased the intratumoral tracer concentration indicating a reduced Pgp transport rate (Fig. 39.3). A problem of the experimental design might be the direct intratumoral injection of drugs which could impair tumor perfusion. However, since in the contralateral tumor the same volume of DMSO was injected, the specific effect of SB203580 can be derived. In all tumors the activity in the SB203580 treated tumor was markedly higher (on average by the factor of 2). In the present study inhibition of ERK1/2 on the Pgp activity had only a minor impact on the Pgp activity which is in good accordance with previous indirect results on chemosensitivity of tumors [6].

The new  $^{68}\text{Ga}$ -labeled tracer is suitable for PET imaging of the tissue Pgp activity. With this tracer it becomes possible to identify patients with multidrug-resistant tumors pre-therapeutically. *In vivo* imaging reveals that tumor acidosis activates the Pgp markedly, a mechanism in which the p38-MAPK pathway seems to play an important role. From these results new strategies for overcoming multidrug resistance (e.g., increasing tumor pH, inhibition of p38) may be developed.

**Acknowledgments** This study was supported by Deutsche Krebshilfe (grants 106774/109136).

## References

1. Vaupel P, Kallinowski F, Okunieff P (1989) Blood flow, oxygen and nutrient supply, and metabolic microenvironment of human tumors: a review. *Cancer Res* 49:6449–6465
2. Mueller-Klieser W, Vaupel P, Streffer C (1998) Energy status of malignant tumors in patients and experimental animals. In: Molls M, Vaupel P (eds) *Blood perfusion and microenvironment of human tumors*. Springer, Berlin, pp 193–207
3. Sanna K, Rofstad EK (1994) Hypoxia-induced resistance to doxorubicin and methotrexate in human melanoma cell lines *in vitro*. *Int J Cancer* 58:258–262
4. Schinkel AH, Jonker JW (2003) Mammalian drug efflux transporters of the ATP binding cassette (ABC) family: an overview. *Adv Drug Deliv Rev* 55:3–29
5. Fojo T, Bates S (2003) Strategies for reversing drug resistance. *Oncogene* 22:7512–7523
6. Sauvant C, Nowak M, Wirth C et al (2008) Acidosis induces multi-drug resistance in rat prostate cancer cells (AT1) *in vitro* and *in vivo* by increasing the activity of the *p*-glycoprotein via activation of p38. *Int J Cancer* 123:2532–2542

- 212 7. Thews O, Gassner B, Kelleher DK et al (2006) Impact of extracellular acidity on the activity  
213 of p-glycoprotein and the cytotoxicity of chemotherapeutic drugs. *Neoplasia* 8:143–152
- 214 8. Zhernosekov KP, Filosofov DV, Baum RP et al (2007) Processing of generator-produced  $^{68}\text{Ga}$   
215 for medical application. *J Nucl Med* 48:1741–1748
- 216 9. Kunikane H, Zalupski MM, Ramachandran C et al (1997) Flow cytometric analysis of  
217 p-glycoprotein expression and drug efflux in human soft tissue and bone sarcomas. *Cytometry*  
218 30:197–203
- 219 10. Thews O, Wolloscheck T, Dillenburg W et al (2004) Microenvironmental adaptation of experi-  
220 mental tumours to chronic vs acute hypoxia. *Br J Cancer* 91:1181–1189

Uncorrected Proof